95 GHz Metamorphic HEMT Power Amplifiers on GaAs

Katherine J. Herrick, Steven M. Lardizabal, Phil F. Marsh, Colin S. Whelan

Raytheon RF Components, 362 Lowell St., Andover, MA 01810 USA

Abstract — **This paper reports on the first 95 GHz metamorphic HEMT power amplifier demonstration including power as a function of temperature. Two power MHEMT materials with 53% and 53%/43% indium channels are investigated showing a slight advantage to the split channel material. At 95 GHz, Gmax values ranging 8.25-10.8 dB are shown for both materials. Single stage 0.15 mm periphery amplifiers using single 4 x 37.5 μm FETs show > 10 dB small signal gain. Two dB compressed power data at 95 GHz yields 15.3 dBm (224 mW/mm) and PAEs up to 22.8%. Increasing temperature up to 80C results in output power and PAE degradation of only 0.43 dB and 2.6 percentage points, respectively. These promising results are on the path to 100-300 mW MHEMT power amplifiers at W-band with improved manufacturability over InP HEMT.**

I. Introduction

For high frequency power applications through W-band, the device trend has been toward improved channel confinement, higher electron mobility, shorter gate lengths, and higher breakdown voltage. Thus far these goals have been best met with InP HEMT due to its superior carrier transport characteristics and carrier confinement [1]. This is primarily due to the 53% high indium content InGaAs channel, which is lattice-matched to the InP substrate. In fact, the best 95 GHz power amplifier (PA) to date is a two-stage InP HEMT PA with 1.28 mm output periphery yielding 427 mW power out and 19% efficiency from 1998[2]. Despite this success, commercialization of InP-based PAs have been limited by the fragility, small wafer size, and low volume InP substrates resulting in high cost per PA and poor reliability.

Metamorphic HEMT or MHEMT allows a range of InGaAs channel compositions (30-80%) to be grown on GaAs substrates with a compositionally graded buffer layer (~1 um). Although MHEMT offers a cost and manufacturability improvement over InP[3], its true advantage is the ability to tailor the In_XGaAs composition for each application. Thus far GaAs-based MHEMT has shown exceptional millimeter-wave, low noise amplifier performance from 35 GHz[4] into W-band[5], and the reliability (~10^6 MTTF at 125C) to compete with InP HEMTs[6].

In this paper, the first 95 GHz MHEMT power amplifier technology is presented including measured gain, power, and efficiency over temperature. Two approaches for power MHEMT devices are investigated with the predominant differentiators being 1) a 53% indium InGaAs channel replicating InP HEMT perfomance and 2) a composite 53%/43% indium InGaAs channel for improved breakdown voltage. In addition to an array of test FETs, two single stage amplifiers are designed around 0.15 mm MHEMT devices with different matching networks (load targets). Both the single and split channel power MHEMT technologies are applied to these circuits, and show that MHEMT is prepared to rival the best InP HEMT in W-band power performance with high manufacturability.

II. MHEMT Material Growth and Fabrication

The power MHEMT material growth and processing are variants of Raytheon's standard low noise MHEMT with 60% indium in the channel and 0.15 um gate length. On 50 um substrates, typical mobility levels are >10,000 cm^2/Vs with transconductance values of 1000 mS/mm and Imax of 830 mA/mm. Typical drain-source voltage operation for this standard material is 1.5V which allows for state-of-the-art low noise amplifier performance through W-band but prohibits power amplifier performance due to its low on-state breakdown.

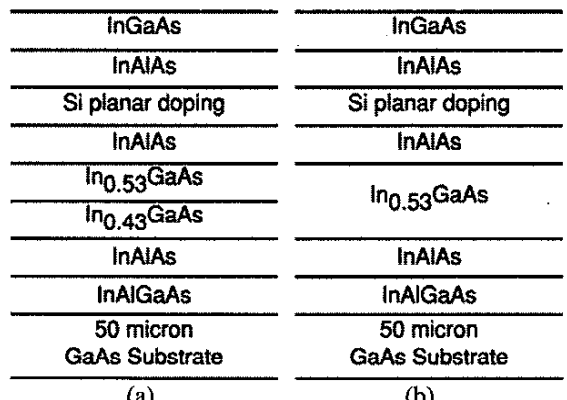

Fig. 1. Epitaxial layer structure for (a) split channel and (b) single channel power MHEMT material.

0-7803-7695-1/03/$17.00 © 2003 IEEE

To improve on-state breakdown voltage and thus operating voltage, a number of adjustments have been made to both material growth and processing. The new power MHEMT material has reduced indium in both the single (53%) and split channel (53%/43%) versions. Reduced passivation and InGaAs layer have also been employed. Fig. 1 shows the epilayer stackup for split channel and single channel W-band power MHEMTmaterial.

III. DEVICE CHARACTERIZATION

Mobility, transconductance, and Imax for 60%, 53%, and 53%/43% devices are shown in Table 1. Note that mobility is $\geq$ 9000 cm^2/Vs and that on-state breakdown voltage (Igs=0.2 mA/mm @ Ids=150mA/mm) has been improved significantly to operate at 2.5V.

TABLE I. SUMMARY OF DEVICE CHARACTERISTICS

Channel % In	**60%**	**53%**	**53%/43%**
Mobility (cm^2/Vs)	10000	9600	9000
Transconductance (mS/mm)	1000	850	820
Imax (mA/mm)	830	700	660
On state Breakdown/Burn out voltage (V)	1.5V/3 V	2.2V/6 V	2.5V/8V

DC and pulsed IV data is shown for a 4 x 37.5 μm device from the split channel power MHEMT material in Fig. 2. Drain-source current in mA/mm is plotted against drain-source voltage up to 4 volts. Gate-source voltage is plotted in 0.1 V steps from -1V to 0.8V. Pulsed (2.5 Vds, 200 mA/mm quiescent bias) and DC data are superimposed showing agreement between the two, implying the device is not thermally limited and has a low trap density.

In Fig. 3, pulsed IV characteristics of both single (dashed) and split channel (solid) power MHEMT material is compared as drain-source current (mA/mm) versus gate-source voltage at Vds=2.5V. For a given gate-source voltage the split channel material operates at a slightly higher current up to 0.5 Vgs.

An array of FETs ranging from 2 x 37.5 to 10 x 60 um were fabricated and measured. Based on small signal S-parameters after TRL on-wafer calibration, Gmax is calculated and plotted in Fig. 4 at Vds=2.5 V, Ids=30 mA for the collection of test FETs. Gmax ranges from 8.25 dB to 10.8 dB at 95 GHz. Some general observations are additionally made from Fig. 4: 1) As the number of fingers increases from 2 to 10, Gmax is reduced. 2) Shorter gate widths yield higher Gmax values. 3) Generally, the split channel (solid line) data yields higher Gmax values than the single channel (dashed). Some of the variation in the data may be attributed to calibration.

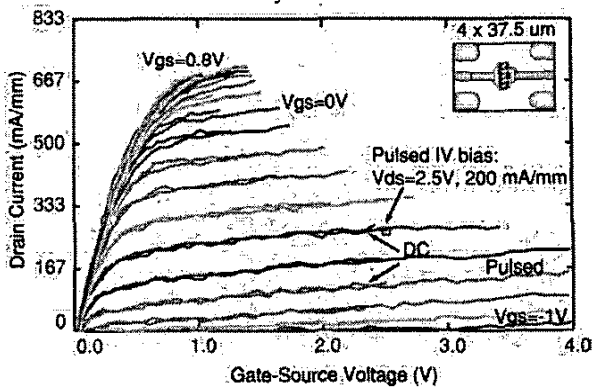

Fig. 2. Pulsed and DC drain current (mA/mm) versus drain-source voltage (V) for the split channel power MHEMT materials.

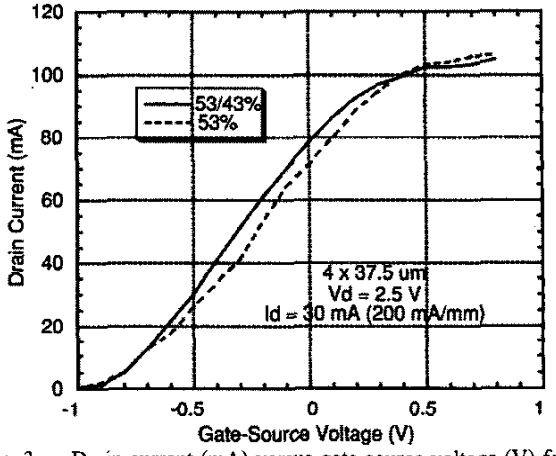

Fig. 3. Drain current (mA) versus gate-source voltage (V) for both single (dashed) and split channel (solid) power MHEMT materials.

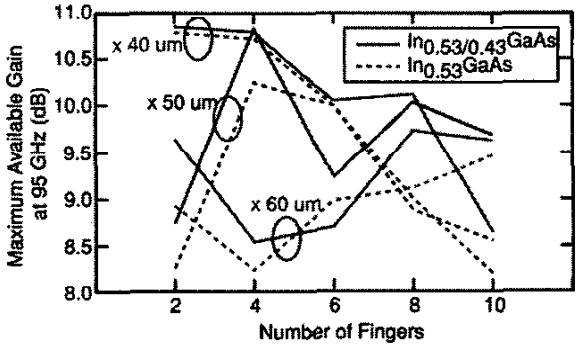

Fig. 4. Maximum available gain at 95 GHz for an array of test FETs ranging 2 fingers by 40 μm to 10 fingers by 60 μm for

both single (dashed) and split channel (solid) power MHEMT material.

IV AMPLIFIER DESIGN

Single stage, 95 GHz, microstrip amplifiers are designed around 4x37.5μm small signal device models created from standard (60% In) MHEMT measurements. Load line analysis from pulsed IV data is used for power design. Table 2 represents the range of load targets used for each single stage amplifier. Power estimates range 15-40 mW or 105-270 mW/mm. Coupled line input/output matching networks are designed extensively with electromagnetic simulation to account for high frequency parasitics. The impedance loads materialized through the different matching networks are used to capture trade-offs between power, gain, and efficiency. DC bias is provided through separate gate and drain lines.

TABLE 2.
SINGLE STAGE AMPLIFIER LOAD TARGETS (0.15 MM FET)

Load Line	Power Density (mW/mm)	Power Estimate (mW)	Ropt (Ω*mm)	Copt (pF/mm)
1	105	16	1.7	0.6
2	180	27	4	0.6
3	270	40	6	0.6
4	173	26	9.9	0.6

V AMPLIFIER PERFORMANCE

In this section, two single stage amplifier designs are evaluated on both split channel (53%/43%) and single (53%) channel power MHEMT material. The difference between the two designs, referred to as ckt1 (Fig. 5) and ckt2 (Fig. 6), are the input and output matching sections. Ckt1 is gain matched and ckt2 is power matched with load line 1 from Table 2.

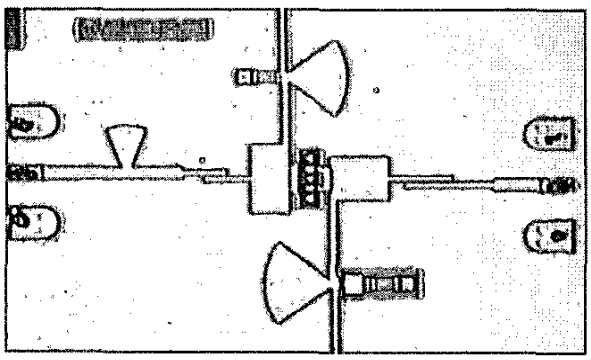

Fig. 5. Photograph of single stage amplifier (ckt1) with 4 x 37.5 μm FET with separate DC gate and drain bias.

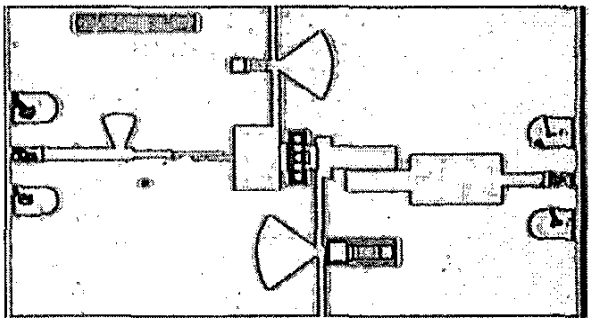

Fig. 6. Photograph of single stage amplifier (ckt2) with 4 x 37.5 μm FET with separate DC gate and drain bias.

A. Small signal s-parameters

Small-signal s-parameter measurements are taken using the Agilent 8510XF network analyzer. With 1 mm coaxial cables and TRL calibration standards from 2-110 GHz, measured results are taken in one sweep from 2-110 GHz. Fig. 7 shows typical measured s-parameter data from ckt1. This 0.15 mm periphery amplifier exhibits over 10 dB of small signal gain at 95 GHz at a bias of 2.5V, 200 mA/mm. S_{11} and S_{12} are at –15 dB at 95 GHz.

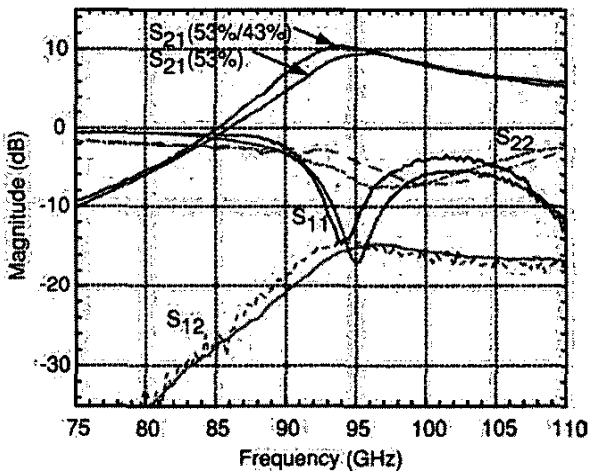

Fig. 7. Measured s-parameters from ckt1 on both single and split channel power MHEMT material.

B. Power and Temperature

Power measurements are taken using a 95 GHz source with a calibrated waveguide-based power bench operating at CW. Measured output power, gain, and power added efficiency (PAE) are shown as a function of input power for ckt1 from the split channel power MHEMT material in Fig. 8. Three separate ckt1 amplifiers are measured and superimposed. At 3 dB compression, output power levels for the three circuits are 13.84 dBm, 14.22 dBm, and

14.26 dBm. Three dB compressed gain is 5.23 dB, 5.27 dB, and 5.88 dB. PAE ranges 22.6% to 22.8%.

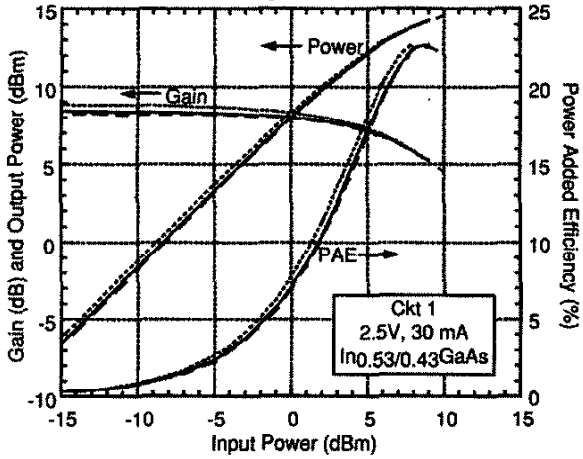

Fig. 8. Measured output power, gain, and efficiency as a function of input power for ckt1 single stage amplifier on split channel material. Three separate amplifier measurements are superimposed.

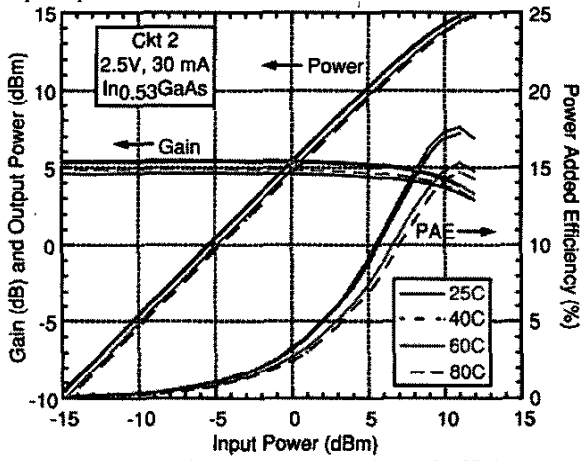

Fig. 9. Measured output power, gain, and efficiency as a function of input power and temperature for ckt2 single stage amplifier on single channel material.

Measured output power, gain, and power added efficiency (PAE) is shown as a function of input power and temperature for ckt2 from the single channel power MHEMT material in Fig. 9. Measurements are taken at 25C, 40C, 60C, and 80C. At 80C and 2 dB compression, 95 GHz output power has reduced by 0.43 dB to 14.84 dBm and PAE has reduced minimally by 2.6 percentage points resulting in a 14.5% PAE. At room temperature, this device produces 15.27 dBm or 224 mW/mm, with 17% PAE. Compared to ckt1 in Fig. 8 (gain-matched), ckt2 is power matched at a potentially non-optimal power load for this MHEMT material. Even better power performance may be achieved with a different load target.

VI CONCLUSION

In summary, this paper shows the first W-band MHEMT power amplifier development including power as a function of temperature at 95 GHz. Split channel (53/43%) and single channel (53%) MHEMTs are compared, with both IV and power data showing stability over temperature. Single stage amplifier results show >10dB small signal gain, while at 2-dB compression, power levels of 224 mW/mm and 23% PAE at 95 GHz are demonstrated. MHEMT amplifier technology is well-positioned and on the path to rival InP HEMT at W-band with improved manufacturability.

ACKNOWLEDGEMENT

The authors wish to acknowledge the assistance and support of our MHEMT measurement team: Steve Lichwala, Ciro Alfaro, Jeff Kotce, and David Loo. In addition, a special thank you to Dr. Michael Adlerstein, Defense Technical Director, and Dr. Thomas Kazior, Defense Advanced Technology Development Head.

REFERENCES

[1] C. Nguyen, M. Micovic, "State-of-the-art of GaAs and InP power devices and amplifiers," IEEE Transactions on Electron Devices, Vol 48, No.3, pp. 472-378, Mar 2001.

[2] D.L. Ingram, Y.C. Chen, J. Kraus, B. Brunner, B. Allen, H.C. Yen, K.F. Lau, "A 427 mW, 20% compact W-band InP HEMT MMIC power amplifier," *Radio Frequency Integrated Circuits (RFIC) Symposium Proc.*, pp. 95-98, 1999.

[3] W.E. Hoke, T.D. Kennedy, A. Torabi, C.S. Whelan, P.F. Marsh, R.E. Leoni, J. H. Jang, I. Adesida, K.L. Chang, K.C. Hsieh,"Properties of metamorphic materials and device structures on GaAs substrates," Int. Conf. On MBE, pp.69-70, 2002.

[4] C.S. Whelan, P.F. Marsh, W.E. Hoke, R.A. McTaggart, P.S. Lyman, P.J. Lemonias, S.M. Lardizabal, R.E. Leoni III, S.J. Lichwala, T.E. Kazior, " Millimeter-wave low-noise and high power metamorphic HEMT amplifiers and devices on GaAs substrates," *IEEE Journal of Solid State Circuits*, Vol. 35, Iss. 9, pp. 1307-1311, Sept 2000.

[5] K.C. Hwang, P.C. Chao, C. Creamer, K.B. Nichols, S.Wang, D. Tu, W. Kong, D. Dugas, G. Patton, "Very high gain millimeter-wave InAlAs/InGaAs/GaAs metamorphic HEMT's," *IEEE Electron Device Letters*, Vol. 20 Issue: 11, pp. 551 –553, Nov 1999.

[6] P.F. Marsh, C.S. Whelan, W.E. Hoke, R.E. Leoni III, T.E. Kazior, "Reliability of metamorphic HEMTs on GaAs substrates," *GaAs Reliability Workshop Proceedings*, pp. 119-132,200